

LA-UR-96- 2832

Title: **High-Temperature Superconducting
Conductors and Cables**

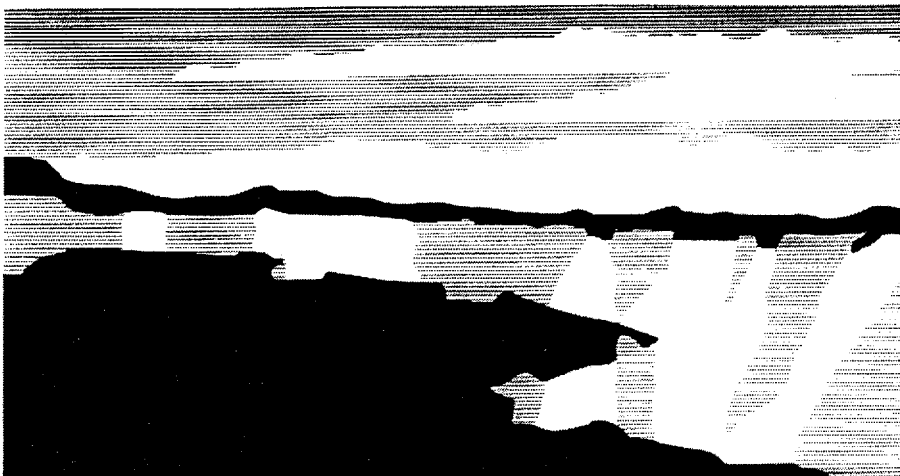
Author(s): **Dean Peterson, STC
Martin Maley, STC
Lev Boulaevskii, T-11
Jeffrey Willis, STC
J. Yates Coulter, STC
John Ullmann, P-23
Jin Cho, STC
Steven Fleshler, STC**

RECEIVED
SEP 09 1996
OSTI

Submitted to: **DOE Office of Scientific and Technical
Information (OSTI)**

MASTER

Los Alamos
NATIONAL LABORATORY



Los Alamos National Laboratory, an affirmative action/equal opportunity employer, is operated by the University of California for the U.S. Department of Energy under contract W-7405-ENG-36. By acceptance of this article, the publisher recognizes that the U.S. Government retains a nonexclusive, royalty-free license to publish or reproduce the published form of this contribution, or to allow others to do so, for U.S. Government purposes. The Los Alamos National Laboratory requests that the publisher identify this article as work performed under the auspices of the U.S. Department of Energy.

Form No. 836 R5
ST 2629 10/91

DISTRIBUTION OF THIS DOCUMENT IS UNLIMITED

RB

DISCLAIMER

**Portions of this document may be illegible
in electronic image products. Images are
produced from the best available original
document.**

DISCLAIMER

This report was prepared as an account of work sponsored by an agency of the United States Government. Neither the United States Government nor any agency thereof, nor any of their employees, makes any warranty, express or implied, or assumes any legal liability or responsibility for the accuracy, completeness, or usefulness of any information, apparatus, product, or process disclosed, or represents that its use would not infringe privately owned rights. Reference herein to any specific commercial product, process, or service by trade name, trademark, manufacturer, or otherwise does not necessarily constitute or imply its endorsement, recommendation, or favoring by the United States Government or any agency thereof. The views and opinions of authors expressed herein do not necessarily state or reflect those of the United States Government or any agency thereof.

High-Temperature Superconducting Conductors and Cables

Dean E. Peterson*, Martin P. Maley, Lev Boulaevskii, Jeffrey O. Willis,
J. Yates Coulter, John L. Ullmann, Jin Cho, and Steven Fleshler

Abstract

This is the final report of a three-year, Laboratory-Directed Research and Development (LDRD) project at the Los Alamos National Laboratory (LANL). High temperature superconductivity, HTS, promises more efficient and powerful electrical devices such as motors, generators and power transmission cables. Their economic viability and widespread use depends on developing HTS conductors that sustain high current densities, J_c , in substantial magnetic fields at temperatures approaching the boiling point of liquid nitrogen, where refrigeration economics and reliability are acceptable. Our early work concentrated on copper oxides but at present, long wire and tape conductors can be best manufactured from BSCCO compounds with high J_c at low temperatures, but which suffer severe degradation at temperatures of interest. This problem is fundamental to BSCCO compounds and is associated with thermally activated motion of magnetic flux lines that generate resistive dc losses. Reducing dc losses at higher temperatures will require a high density of microscopic defects that will effectively "pin" flux lines and inhibit their motion. Recently it was demonstrated that optimum defects can be produced by tracks of small dimension formed by passage through the sample of energetic heavy ions. Such defects result when bismuth is bombarded with high energy protons. The longer range of protons in matter suggests the possibility of application to tape conductors. AC losses are a major limitation in many applications of superconductivity such as power transmission. The improved pinning of flux lines is known to reduce ac losses, but optimization also involves other factors. The measurement and characterization of these losses with respect to material parameters and conductor design is essential to successful development of ac devices.

*Principal contact, e-mail: dpeterson@lanl.gov

1. Background and Research Objectives

The relationship between structural and electronic properties has emerged as a key issue in interpreting the normal-state properties, the mechanism of HTS, and the shortcomings in performance of the materials. Special attention has been given those techniques sensitive to the local structure of materials since our work has indicated a qualitative variation of crystallographic structure at the mesoscopic scale relative to the global structure determined by conventional x-ray or neutron-diffraction techniques. Two techniques particularly well suited for these studies are NMR/NQR and pair-distribution function (PDF) analysis of diffraction data, both of which have been used extensively. As needed these are complemented by more conventional magnetic susceptibility, x-ray and neutron-diffraction, resonant ultrasound, electrical resistance, thermal expansion, low-temperature specific heat, critical current (to 1000 Amperes), ac loss, electron microscope, and high-temperature thermodynamic measurements. Precise many-body models have been developed that combine magnetic correlations with electron-lattice and charge-transfer degrees of freedom. Models and techniques employed include multi-dimensional Hubbard models, unrestricted Hartree-Fock, and exact diagonalization methods. A time-dependent equation for the inter-layer phase differences was derived for Josephson-coupled layered superconductors. These models in turn suggested new experiments such as an NMR technique to follow the structure of the moving vortex state in real materials.

BiSrCaCuO (BSCCO) Tapes

At present there is only one HTS group of compounds, the BiSrCaCuO (BSCCO) system, that has been successfully made into long continuous lengths of wires and tapes that carry high current density without interruption by intergranular weak links. Several groups have reported achieving critical current density, J_c , values greater than 10^5 A/cm² at 4.2 K in fields up to 25 T in tape conductors based on both the Bi₂Sr₂CaCu₂O_x and the (Bi, Pb)₂Sr₂Ca₂Cu₃O_y compounds (Bi-2212 and Bi-2223, respectively), and prepared by the oxide-powder-in-tube (OPIT) process. Recently, these OPIT tapes have been manufactured in lengths of 1000 m with properties comparable to those of short samples. Unfortunately, this system of compounds is severely limited by thermally activated motion of magnetic flux lines out of pinning centers provided by microscopic defects. This activated flux motion (flux creep) generates ohmic dissipation and limits operation of BSCCO-based conductors to the H-T region below the "irreversibility line" ($T_{irr} \sim 35$ K for $H \sim 1$ T). To stabilize currents with low dissipation at higher temperatures will require defect structures with much higher pinning strength. Recent success with columnar defects produced by heavy ion irradiation at high

energy has shown that linear tracks with well defined radii of 5-7 nm are the most effective in pinning flux lines and that T_{irr} for Bi-2212 can be raised by ~20 K with an optimum density of tracks. Unfortunately, heavy ions have a maximum range in solids of only 20-30 μm , making this an impractical technique for application to OPIT tapes in which the BSCCO core is encased in a Ag sheath 20-40 μm thick.

It was recently demonstrated that randomly oriented columnar tracks can be created in situ throughout the bulk of a thick Bi-2212 film by heavy fission fragments that result when 0.8 GeV protons collide with Bi nuclei. The large range of these high energy protons (~0.5 m) and the large cross section for fission of high-Z nuclei make it possible to generate dense arrays of columnar tracks throughout the interior of bulk conductors and even large scale devices such as solenoids. It has been predicted that these splayed columnar tracks are even more effective in reducing flux motion than the parallel ones produced by heavy ion irradiation. The previous demonstration of this technique was carried out on 3-4 μm thick films of Bi-2212 deposited onto Ag substrates and showed significant enhancement of magnetic hysteresis loops, the irreversibility line and magnetization J_c values at high temperature and high field. An investigation was undertaken to test the effect of 0.8 GeV proton irradiation on transport current densities obtained directly from current-voltage characteristics measured on standard OPIT Bi-2223/Ag tape conductors. The study demonstrates the feasibility of penetrating the Ag sheath and thicker (~30 μm) BSCCO core. Most importantly, this work shows that the resulting columnar defects produce positive and significant enhancements of bulk transport currents in substantial applied magnetic fields for these polycrystalline materials.

2. Importance to LANL's Science and Technology Base and National R&D Needs

The performance of HTS is severely limited at high temperatures by thermally activated flux motion. The source of this problem is embedded in novel aspects of the HTS compounds and its solution presents challenges of both a technical and a scientific character. Since the discovery of HTS in 1987, LANL has played a leading role in the technology development in collaboration with U. S. industry, with the aim of producing more powerful and efficient electrical devices. This project takes a promising new approach to solving a critical problem blocking the widespread use of HTS technology.

3. Scientific Approach and Results

This report integrates the results of three years of effort where considerable progress has been made in several areas. The work is both theoretical and experimental. We have undertaken studies to integrate theoretical modeling and physical measurements with sample synthesis in order to relate magnetic flux pinning to phase behavior, crystalline anisotropy, and texture development.

Theoretical Work on Cuprates

Realistic theoretical descriptions are proving essential for guiding new experiments and extracting materials parameters. We have exactly diagonalized a model Hamiltonian based on both electron-electron and electron-phonon coupling for the O-Cu-O cluster in YBCO. It is impressive that the calculated results agree with conclusions from EXAF, infrared, Raman, and neutron scattering measurements. The position of crystal field excitons in La-214 were predicted using a cluster model and the results verified experimentally by resonance Raman experiments at the University of Illinois. We have continued to phenomenologically model possible mechanisms which limit the critical current in HTS tapes. It was concluded that in Bi-2223 tapes, the limitation is imposed by very weak coupling between the main part of the grains and by the magnetic field pinning mechanism inside strongly coupled grains. The anisotropy of critical currents in Bi-2223 tapes was also successfully theoretically modeled. Effects of vortex fluctuations in the NMR frequency shift and linewidth in the Bi- and Tl-based HTS was shown to be significant. The temperature and magnetic field dependence of Bi-2223 was explained within the framework of high-field scaling theory.

A wide variety of unusual structural properties were shown to be associated with HTS materials and are very likely at the root of these novel and technologically important materials. We have utilized a wide variety of sophisticated probes of local crystallographic structure, electronic structure, and magnetism in cuprates and related them to produce a microscopic understanding of the materials. Novel techniques employed in these studies included nuclear magnetic resonance, nuclear quadrupole resonance, resonant ultrasound spectroscopy, thermal expansivity, flux flow noise, neutron and X-ray diffraction, photoemission spectroscopy, magnetometry, heat capacity, Rutherford backscattering, and Mossbauer spectroscopy. An unusual sensitivity of local structure in metallic, oxygen doped La-214 to the presence of enough doped holes to produce superconductivity was demonstrated. Photoemission spectroscopy showed strong anisotropy in the superconducting energy gap in Bi-2212 consistent with d-wave symmetry of the order parameter. Analysis of flux flow noise indicated a wide distribution of pinning energies and that very large bundles of fluxoids move together at

low temperatures. All nine of the elastic constants were determined by RUS for a detwinned YBCO single crystal. The flow of current through Bi-2223 tapes has been investigated as a function of temperature and orientation within a magnetic field. The results were successfully phenomenologically modeled.

Thick YBCO films (>5 microns) with high critical current densities, [$J_c(77K) > 1 \text{ MA/cm}^2$] have been fabricated by pulsed laser deposition. YBCO thin films (4000 Å) with comparable J_c values have also been deposited on nickel metal by using an intermediate buffer layer aligned by depositing with simultaneous ion bombardment. Thin films of SrRuO₃ and La_{0.5}Sr_{0.5}CoO₃ were grown epitaxially on Pt/MgO layered substrates in order to fabricate a low resistivity electrode for use in ferroelectric capacitors. The room temperature resistivity of 40 micro-ohm.cm is the lowest ever reported in the literature. Multilayers of SrRuO₃/YBCO thin films were also successfully fabricated for use in developing SNS junctions. YBCO films were successfully grown on LiNbO₃ substrates without the use of buffer layers. Such a multilayered assembly could be very useful in electro-optic devices. High quality YBCO thin films were fabricated on low dielectric constant, low loss tangent MgF₂ with buffer layers which opens new possibilities for HTS applications at high frequencies. The Hall angle in YBCO epitaxial thin films was studied as a function of oxygen reduction and Pr doping.

Theoretical Modeling

Experimental evidence supports the importance of local structure or "texture" in high-temperature superconductors. It is now clear that specific mesoscale textures and their associated slow dynamics are correlated strongly with macroscopic superconductivity. Important relationships between structural and spin (electronic) properties have been revealed so that, although the question of which of many is the principal superconducting pairing mechanism awaits further experiments, the need to include local dynamic lattice degrees-of-freedom is evident. The highly polarizable oxygens, both in the Cu-O planes and in the anomalous c-axis direction, are especially implicated. Therefore, we have closely studied the theory and modeling of coexisting electron-lattice and electron-electron interactions. (1) We find that doping holes, necessary for superconductivity, into antiferromagnetic stoichiometric states results in polaronic lattice-distortion signatures in IR and Raman spectroscopies, as observed in chemical- and photo-doping experiments. (2) We have introduced a model for polaronic charge-transfer in the interlayer c-axis direction, which provides a microscopic model of short-range polarizability of the material lying off the principal Cu-O planes. This model is solved by exact diagonalization numerical methods. It is able to correlate both structural and optical signatures of nonlinear and, in general, nonadiabatic behavior consistent with experiments probing the Cu-O bond length and dynamics. In particular, we have shown the

need to develop energy-resolved pair-distribution probes, a technology which is now possible with pulsed neutron sources. (3) We have shown that an anharmonic electron-lattice interaction model can explain observations in the far IR of extremely anomalous c-axis oxygen phonon modes (oscillator strengths, damping, line-shape), where the anharmonicity results from coupling to spin degrees-of-freedom. (4) Finally, we have shown that spin-Peierls and superlattice ground states are intrinsic to low-dimensional, multi-band Peierls-Hubbard models that characterize cuprate superconductors.

Theoretical calculations and growing experimental evidence suggest that the Fermi surface of $\text{La}_{2-x}\text{Sr}_x\text{CuO}_4$ consists of hole pockets for small x . It was not understood how this Fermi surface evolves at larger x into a large electron-like surface. We have answered this question using mean-field and more sophisticated methods and can now for the first time explicitly describe the evolution of the Fermi surface from small to large x . As antiferromagnetic, long-range order weakens and disappears, the hole pockets elongate and merge, and the discontinuity in $\langle n_{\mathbf{k}} \rangle$ farthest from the G point also vanishes. Some subtleties in interpreting photoemission experiments were also discovered.

Considerable effort has been devoted to the study of the Hubbard model and related magnetic models, such as the Heisenberg model, in an attempt to understand the physical properties of the high-temperature superconductors. Using the 1-D Hubbard model, we have investigated the nature of the metal-insulator transition in one dimension as a function of the doping. In leading order we find that the chemical potential is a quadratic function of the doping. This is not typical behavior for a Fermi liquid, as expected in 1-D since Fermi liquid theory breaks down in this dimension. In our study of the 2-D Hubbard model we have found some surprising numerical results from the work of Furukawa and Imada. They find that the chemical potential also is a quadratic function of the doping. While some questions can be raised regarding the numerical methods of this group, there are no obvious problems with their results. We have explored several possible explanations for this behavior in the 2-D system, including extended van Hove singularities and doping in the presence of a mean-field antiferromagnetic ground state.

At half filling the 2-D Hubbard model reduces to the Heisenberg model. We have studied the behavior of frustrated 2-D Heisenberg models. This type of frustration arises in Sr-doped La_2CuO_4 , when the added charge carriers are trapped on a Sr donor and cause ferromagnetic interactions within the antiferromagnet. We have calculated the spin stiffness exactly as a function of J_1/J_2 for 14-, 16-, and 20-site chains as well as a 4x4 and 4x5 square lattice. The spin stiffness is a measure of the long-range magnetic order in these models. As expected, the increase of the frustration by increasing J_2 eventually destroys the long-range

order. These are exact numerical results that can be used as a test for future calculations and approximation methods.

A concentrated effort has been made to investigate the effects of local "imperfections" on the superconducting and transport properties. (1) The effect of finite-range impurities on the microwave conductivity of cuprates indicates that the conductivity should be nonuniversal, as observed experimentally. (2) The wavefunction of an impurity-bound state in a d-wave superconductor is found to be strongly anisotropic and implies the need to revise the standard approach used thus far for analysis of the finite-contribution problem. (3) We have identified the order parameter, which is a Cooper pair and a spin-boson, for odd-gap superconductors. This has allowed us to generate a Ginsburg-Landau theory for odd-gap superconductivity, which may be realized in HTS.

Experimental Work on Cuprates

Much of the direction for theoretical modeling has come from experimental studies sensitive to the local, mesoscale structure in cuprates, particularly those having a single Cu-O plane, e.g., $\text{La}_2\text{CuO}_{4+x}$ and $(\text{La}, \text{M})\text{CuO}_4$ where $\text{M} = \text{Ba}$ or Sr . In the case of $\text{La}_2\text{CuO}_{4+x}$ with $x = 0.03$, NQR measurements show clearly that near $T = 265$ K, mobile excess oxygen atoms separate into a nearly stoichiometric ($x \approx 0.01$) antiferromagnetic phase and an oxygen-rich metallic superconducting phase. An important conclusion is that the phase separation is driven by an electronic mechanism and not by a structural change. Copper NQR spectra of the superconducting phase clearly indicate the presence of two distinct Cu sites, which is not observed by conventional crystallography. For equivalent hole doping, the NQR frequency of these features agrees very well with similar peaks in $\text{La}_{2-x}\text{Sr}_x\text{CuO}_4$, although this material also should have only a single Cu site. Therefore, this effect is independent of the type of dopant (excess oxygen or substitutional Sr) and indicates a change in local structure from the crystal response to doped holes. A preliminary analysis of recent La-NMR data identifies the origin of the unexpected second Cu site in the metallic phase of $\text{La}_2\text{CuO}_{4+x}$ as being one adjacent to CuO_4 plaquettes occupied by a pinned (static) hole donated by the excess oxygen. Our view of this is that interstitial oxygen orders into striped domains by taking advantage of openings in the La-O layers caused by an ordering of CuO_6 octahedral tilts. The second copper site is differentiated by its proximity to stripes of pinned holes formed in the CuO_2 planes. This view is borne out by our recent cluster calculations using a new code developed for this work and explains the observation of a large structural supercell by neutron diffraction in $\text{La}_2\text{CuO}_{4.1}$.

Much attention has been given to the report that bulk superconductivity disappears in $\text{La}_{2-x}\text{Ba}_x\text{CuO}_4$ for $x = 1/8$ and that this disappearance is coincidental with a global structure

change from low-temperature orthorhombic (LTO) to a low-temperature tetragonal (LTT) structure. This transition has been modeled as a rigid tilt of CuO_6 octahedra by 45° about the $[110]$ directions and is accompanied by small strains that distort the octahedra. Using PDF analysis of x-ray diffraction data, we have shown that this is not the case. We find in fact that in both $x = 1/8$ and $x = 0.15$ (a bulk superconductor), the local (coherence length of order 20 Å) structure remains LTT and that the octahedra do not change their local tilt direction at the LTO-LTT transition. An appropriate superposition of the local structure, in which adjacent LTT domains are rotated by 90° does, however, recover the global LTO structure. Thus, the disappearance of superconductivity at $x = 1/8$ is not associated with a change in structure to LTT, but more likely arises from an electronic phase transition. Furthermore within the LTO phase, the structural coherence length found in these measurements is very similar to the superconducting coherence length, electronic mean-free path, and antiferromagnetic correlation length, suggesting that all of these length scales may be related. The PDF analysis of neutron-diffraction data on these materials confirm conclusions from the x-ray data.

Following our discovery of a cooling-rate dependence of the superconducting transition temperature T_c in oxygen doped $\text{La}_2\text{CuO}_{4+x}$, we showed by NQR measurements that this cooling-rate dependence was due to incomplete phase separation, which leaves the metallic phase with lower hole doping. To investigate this, we have studied the cooling-rate dependence of four $\text{La}_2\text{CuO}_{4+x}$ samples in which x was varied systematically. In all cases optimal critical temperatures were found if the sample was "annealed" at $195 \pm 5\text{K}$ but that the maximum T_c increased with increasing x , as expected.

To understand the nature of the antiferromagnetic background in doped La_2CuO_4 , detailed NQR studies were carried out near the Néel temperature (T_N) in $\text{La}_2\text{CuO}_{4+x}$ in which $x \sim 0$. The onset of NQR Zeeman splitting at T_N was found to be abrupt but continuous, indicative of a second-order phase transition with either a crossover in critical behavior just below T_N or a very small critical exponent. The absence of an anomaly at T_N in the electric field gradient or in our thermal expansion measurements indicates no accompanying structural distortion.

Applications

We made substantial technical progress in HTS thin films. We focussed on the fabrication of Josephson junctions (JJs) and SQUIDs with a long term goal of developing sensitive low noise magnetometers. Junction performance is usually measured by calculating the product of the critical current I_c and the normal state resistance R_n . The quality of the fit to a JJ model is also a significant factor, but this is not usually measured numerically. For SQUIDs the figure of merit is modulation depth, the range over which the SQUID voltage

varies while an external magnetic field is ramped by half a flux quantum per area. Across a chip the significant numbers are yield of working devices and standard deviation in the parameters.

In our early work our best junction performance at 77 K was an $I_c R_n$ product of 1-2 mV on a biepitaxial grain boundary device using the sputtered films. The yield, however, was low with only one junction working out of dozens fabricated. Some of the other devices had electrical continuity and worked at lower temperatures. The laser-ablation effort had produced no devices that were clearly junctions. The laser-ablated junctions now have $I_c R_n$ products of order 100 mV, but the yield is up to 100 percent on some chips. The electrical properties vary across the chip by a factor of two, but all of the devices exhibit a Josephson effect. The laser-ablated SQUIDs are producing modulations of several microvolts. The junction performance would lead one to expect better SQUID results in the future. The junctions made from sputtered films now have a typical $I_c R_n$ of order 100 mV and SQUID modulation depth of 10 mV. The best sputtered film based chips had a yield of 100 percent with electrical parameters varying over a factor of two.

At the time these results were the best in the field. The best SQUID results reported by groups at Berkeley, Conductus, and Jülich were with bicrystal junctions and had modulation depths of order 20 mV. There was an additional report from DRA-Malvern, UK of 20 mV in a c-axis via design. However, these technologies do not allow flexibility. The group at IBM has worked extensively with step-edge junctions and has a best result of 10 mV of modulation depth using BSCCO films. The highest $I_c R_n$ products have been reported by NIST-Boulder using a hybrid step-edge/SNS (supercond-normal-supercond) design. However their yield is low, and their results unpublished. Amongst the groups working on SNS junctions the best result (other than ours) was at IBM with 6 mV of modulation.

We developed an ion-beam assisted deposition (IBAD) method for creating a textured buffer layer on metal substrates such as Ni. Textured yttria-stabilized Zirconia (YSZ) buffer layers were deposited on Ni with IBAD. Thick YBCO films deposited by pulsed laser deposition on YSZ/Ni have shown a critical current density of 8×10^5 A/cm² at 75 K, which was a world's record. Used as a conductor, a 1.5-mm thick YBCO film carried a record current of 23 Amperes at liquid-nitrogen temperature. This development opened the possibility for us to apply the method to make long, thick YBCO films on metals with buffer layers for power applications.

We concluded investigation of flux creep and pinning in MPMG-processed YBCO and found correlations between the concentration of 211 phase and the enhancement of pinning and flux-creep activation energies. We conducted an investigation of c-axis current transport in single crystals of Bi-2212 in high-magnetic fields and discovered a decoupling of CuO₂ planes

produced by pancake vortex fluctuations along a line in H-T space. The current-flow paths in Bi-2223/Ag tapes, measured with a new technique in which measurements are taken with current flow across the tape thickness, find a percolative path along inclined a-b planes and avoids c-axis transport. This has important implications for understanding the influence of texture on critical current densities. An investigation of the physical and microstructural limitations to critical currents in BSCCO tape conductors was finished including a study of the effects of temperature, magnetic field, and field angle on J_C . We discovered that only 5 to 10 percent of the tape cross section is not weak linked and that the dependence of J_C on T, B, and Q is caused by thermally activated flux motion within the BSCCO grains.

We investigated the manifestations of vortex fluctuations on physical properties of anisotropic superconductors discovering significant effects on heat capacity, equilibrium magnetization, and the interlayer decoupling. A new research effort at the National High Magnetic Field Laboratory-Los Alamos was begun in which we directed construction of sample probes for J_C and VSM measurements and designed a program for studying properties of HTS in high magnetic fields. We instituted a new research initiative at WNR at LAMPF using high-energy protons to fission Bi nuclei, producing splayed columnar defects that optimize pinning in HTS conductors and significantly increase the operating temperature of superconducting devices. We negotiated arrangements for this project with personnel from Physics Division, IBM, and the American Superconductor Corp., wrote a successful proposal to the LAMPF Users Committee, contributed to an SBIR Proposal with ASC, and designed a series of experiments to demonstrate the potential of this new technique. We also instituted a new experimental program on ac-loss measurements that includes design, construction, testing, and initial data analysis of an experimental apparatus for measuring ac losses on small samples of HTS tapes. This project led to our first ac-loss measurements on BSCCO tape samples.

For HTS thin films we have developed a two-zone annealing process for making Tl-based films. A compound of Tl-2212 phase was selected for this study. At first, precursor films without Tl (a toxic element with a very high vapor pressure) were prepared on substrates using sputtering. Then the films and Tl_2O_3 were placed at different locations, and hence temperatures, inside a two-zone furnace. We successfully reduced the annealing temperature of typically 850 °C used by others to 780 °C for these Tl-2212 films, which is significant for reducing the interaction between the films and substrates. Furthermore, the process will enable us to anneal multilayer samples with diameters up to three inches at the same time as compared to small samples in separate annealing steps used by others. This process can be easily scaled up for manufacturing.

A process was developed to prepare high- T_C thin films on $LiNbO_3$. Because $LiNbO_3$ has special electro-optic properties, the integration of a superconducting thin film with $LiNbO_3$

for processing opens up many possibilities for novel devices. Based upon this process, high quality YBCO films with T_c of 90 K and J_c over 1×10^6 A/cm² at 77 K were prepared for the first time on LiNbO₃.

Layers of vacuum and single-crystal sapphire have been used to fabricate a narrow, low-phase noise microwave filter with a pass band for TE₀₁ mode of 100 MHz centered at 10 GHz. Because of the use of low-loss dielectric and HTS materials, the edges of this filter have very sharp onsets. We have measured a dropoff of over 30 dB at 100 kHz from the central frequency. Such a device can be put to great use in communications.

Recent Work on BiSrCaCuO (BSCCO) Tapes

Results have been obtained on both a monofilament and an 85-filament Bi-2223/Ag tape sample manufactured by American Superconductor Corporation (ASC). Tapes were prepared by packing the powder into cylindrical silver billets, which were deformed into tape using standard deformation techniques, including wire drawing to a hexagonal shape, repacking an 85 filament bundle into a silver tube, wire drawing, and rolling. For monofilament tapes the rebundling step was omitted. The samples were given multiple heat treatments at temperatures between 800 and 830°C in 7.5 percent oxygen with intermediate deformations consisting of pressing for the monofilament tapes and rolling for the multifilament tapes. The final dimensions of the monofilament tape are 100 μm thick by ~3 mm wide with a ~35-40 μm thick core and a 20 percent fill factor. The 85 filament tape has dimensions of 250 μm thick and 2.5 mm wide with filament dimensions of 15 μm thick and 120 μm wide and a 28 percent fill factor. As noted above, because of the very long penetration of the 0.8 GeV protons, it was not necessary to remove the silver coating for the irradiations. The samples were irradiated at the WNR Facility of the Los Alamos Meson Physics Facility (LAMPF) with 0.8 GeV protons at an average beam current of 1.2 μA. The beam has an axially symmetric Gaussian distribution in the density of incident protons with a full width at half maximum of 1.2 cm. The size and position of the beam were monitored both before and after each irradiation by remotely observing a phosphor target, which fluoresces when hit by the proton beam, and which could be placed in the same position as the sample. The irradiations were carried out with the samples in vacuum. The two samples were given approximately equal doses. The total dose received by each sample was determined by studies of the ²²Na activation levels on Al foils placed immediately behind the samples. Other irradiated Al foils were used to determine the distribution of the proton beam intensity more precisely.

The average proton fluences received by each of those sectors of the monocoil tape were 1.6, 2.9 and 7.6 x 10¹⁶ protons/cm². For the multifilamentary tape, measurements were

made on only the sector that received the highest fluence, estimated to be 7.6×10^{16} protons/cm². The number of fissions produced per proton was determined as the product of the proton fluence, the density of Bi nuclei in Bi-2223 (7.33×10^{21} nuclei/cm³), and the Bi fission cross section value of 155 mb at 0.8 GeV interpolated from recent results. The product yields 1.8 , 3.3 and 8.6×10^{13} fissions/cm³ for the monocoil tape sectors and 8.6×10^{13} fissions/cm³ for the multifilamentary tape. Assuming an average track length of 6 μ m for each fission, the real density of tracks is then ~ 1.1 , 2.0 , and 5.2×10^{10} tracks/cm². If the track density is multiplied by the flux quantum f_0 ($= 2.07 \times 10^{-11}$ Tesla-cm²), it can be converted to an equivalent magnetic field B_ϕ , at which the vortex density equals the track density. The concentrations of fission tracks per unit area therefore correspond to matching fields B_ϕ of 0.2, 0.4 and 1.1 T.

For the transport experiments, electrical contacts were soldered onto the tape silver sheath using low-melting-point In-Ag soldering alloy. In all of the experiments reported here, the magnetic field was applied normal to the plane of the tape, that is, parallel to the crystallographic *c* axis for perfectly oriented Bi-2223 grains in the tape. The *I-V* characteristics of the samples were measured with the samples immersed in liquid nitrogen to avoid heating at the contacts. The critical current I_C was determined at an electric field criterion of 1 μ V/cm.

The results of critical current measurements on multi- and monofilamentary tapes are shown in figures 1a and 1b respectively. Both tapes show a remarkable improvement of the transport critical current density after irradiation. This effect is more notable at the higher fields. For example, at 1 T, Figure 1a shows that for the multifilamentary tape J_C has increased from an immeasurably low value to $\sim 5 \times 10^3$ A/cm² at 75K. Also shown in Figure 1a is the magnetic field dependence of the critical current J_C of the irradiated multifilamentary tape at 64 K. Clearly, the fall off in J_C shifts to higher fields at the lower temperature. Furthermore, the 64 K curve of $J_C(H)$ is flatter below the knee, i. e., less dependent on *H*, suggesting that the pinning activation energy increases at lower temperature. Figure 1b shows the transport critical current density J_C normalized to its value at zero field J_{C0} for two different sectors of the irradiated monocoil tape and for an unirradiated ASC monocoil tape at 75 K. Clearly evident is the progressive improvement with radiation fluence of the field dependence of J_C , with the functional form of $J_C(H)$ at the highest fluence matching that of the multifilamentary tape.

In summary, it has been shown that by means of 0.8 GeV proton irradiation it is possible to greatly improve the transport critical current at high temperatures of industrial state-of-the-art, bulk high T_C superconductors in the form of mono- and multifilamentary tapes. All of these results demonstrate that irradiation at these dose levels does not produce weak links,

which would decrease the low field critical current values. Rather, it was found that the transport critical current densities are homogeneously improved throughout the H - T plane. Thus high-energy proton irradiation appears to be an effective technique for enhancing the operating temperature of devices made with BSCCO conductors.

Publications

1. Boulaevskii, Lev; Larkin, Alexi; Maley, Martin; and Vinokur, Valeri, Physical Review Letters, 1995.
2. Maley, Martin; Willis, Jeffrey; Bulaevskii, Lev; Cho, Jin; Safar, Hugo; Wu, Xin; Foltyn, Steven; and Arendt, Paul, "Physical Phenomena at High Magnetic Fields-II," Volume 2, Book Chapter, 1995.
3. Safar, Hugo; Cho, Jin; Fleshler, Steven; Maley, Martin; Willis, Jeffrey; Coulter, James; Ullmann, John; Lisowski, Paul; Riley, Bart; Rupich, Martin; Thompson, James; and Krusin-Elbaum, Lia, Applied Physics Letters, Vol 67, p130, 1995.

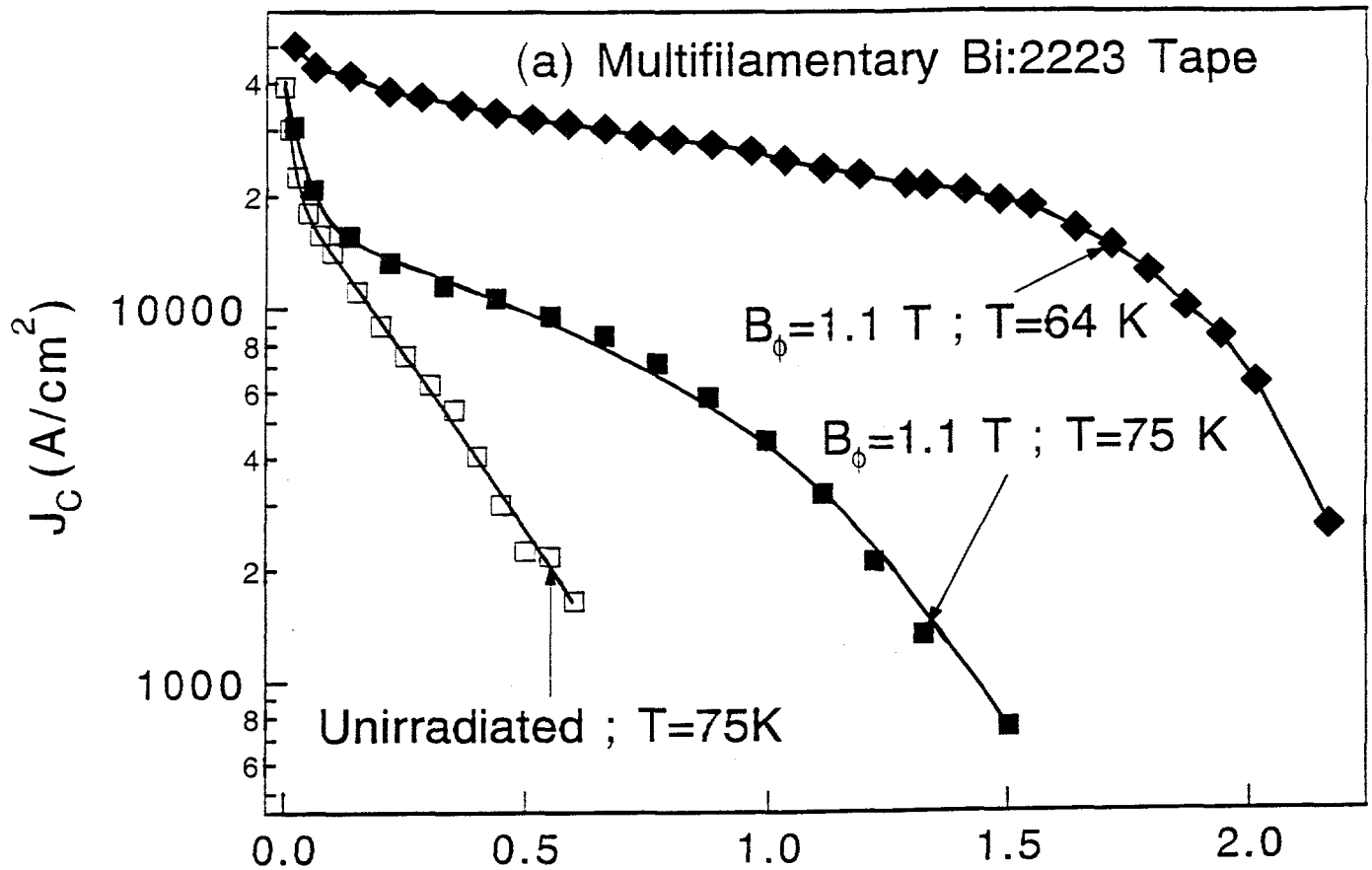


Figure 1a. Critical current density versus magnetic field for the multifilamentary Bi-2223 tape at 75 K in the unirradiated state and after irradiation with 0.8 GeV protons to a fluence corresponding to an estimated matching field of 1.1 T. Data for the irradiated tape is also shown for 64 K.

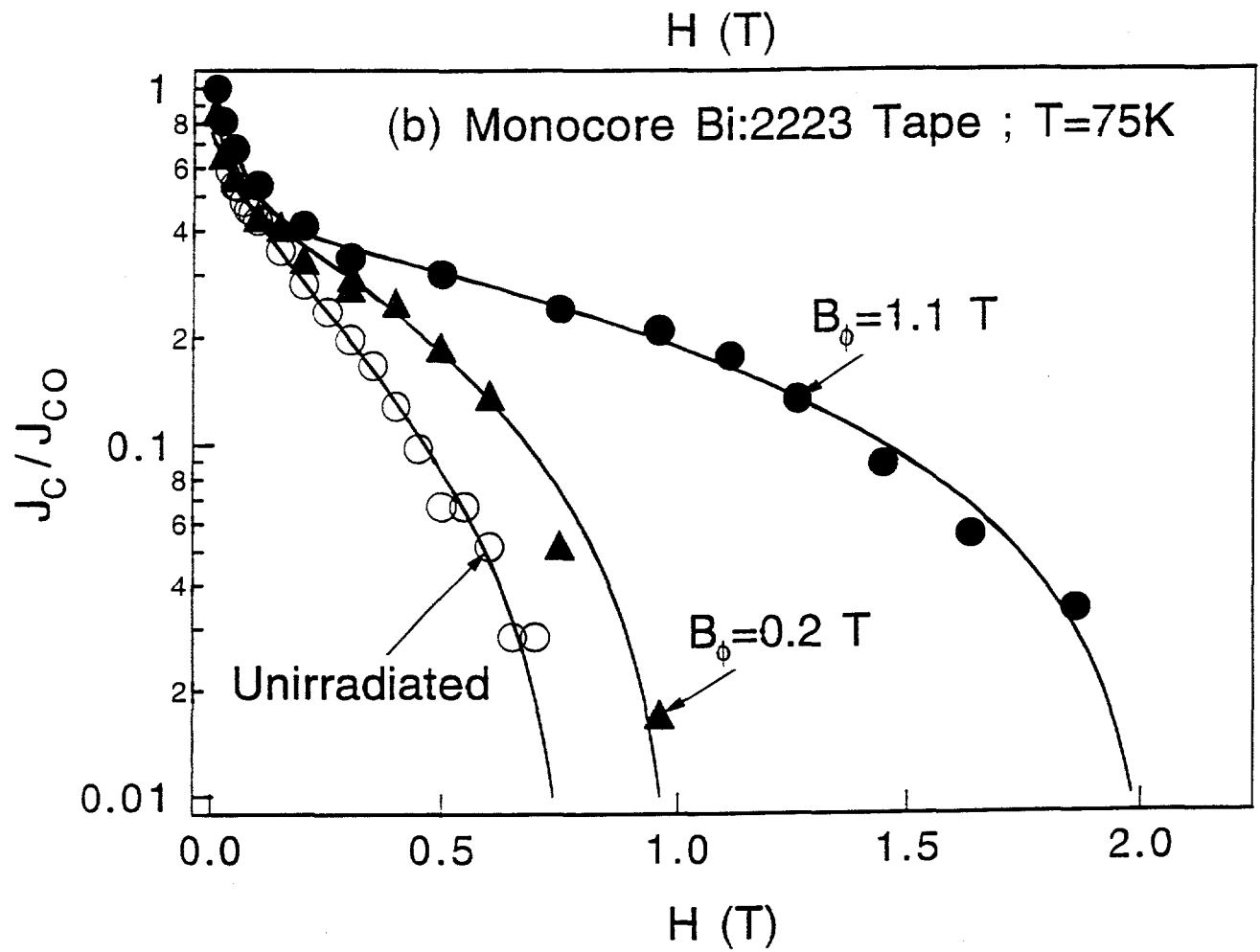


Figure 1b. Normalized critical current density J_c/J_{c0} versus magnetic field at T=75 K for the monocore Bi-2223 tape in the unirradiated state and after irradiation with 0.8 GeV protons at two fluences at different sections of the same piece of tape.